Accepted Manuscript

Catalytic regeneration of Diesel Particulate Filters: Comparison of Pt and CePr active phases

Verónica Rico Pérez, Agustín Bueno-López

PII: S1385-8947(15)00655-5
DOI: http://dx.doi.org/10.1016/j.cej.2015.05.004
Reference: CEJ 13645

To appear in: *Chemical Engineering Journal*

Received Date: 20 March 2015
Revised Date: 30 April 2015
Accepted Date: 2 May 2015

Please cite this article as: V.R. Pérez, A. Bueno-López, Catalytic regeneration of Diesel Particulate Filters: Comparison of Pt and CePr active phases, *Chemical Engineering Journal* (2015), doi: http://dx.doi.org/10.1016/j.cej.2015.05.004

This is a PDF file of an unedited manuscript that has been accepted for publication. As a service to our customers we are providing this early version of the manuscript. The manuscript will undergo copyediting, typesetting, and review of the resulting proof before it is published in its final form. Please note that during the production process errors may be discovered which could affect the content, and all legal disclaimers that apply to the journal pertain.

ACCEPTED MANUSCRIPT

Catalytic regeneration of Diesel Particulate Filters: Comparison of Pt and CePr active phases.

Verónica Rico Pérez, Agustín Bueno-López*

Department of Inorganic Chemistry. University of Alicante, Ap.99, E-03080 Alicante (Spain).

*email: agus@ua.es;Tel. +34 965903538; Fax. +34 965903454
http://personal.ua.es/es/agus

Abstract

Diesel Particulate Filters (DPF) have been loaded with the same amount (0.6 wt. %) of either Pt or an optimized CePr active phase, and an experimental set-up has been designated and used to investigate the catalytic combustion of soot under realistic reaction conditions. Both active phases were stable under reaction conditions, with no evidences of deactivation in consecutive combustion experiments. The presence of H_2O and CO_2 together with NOx and O_2 in the gas mixture slightly delays soot combustion to higher temperatures, but the effect is equal for the Pt and CePr active phases. The mass of soot loaded into the filters had no effect in the catalytic regeneration of the DPFs for soot:catalyst weigh ratios below 0.4, while it was hindered above this ratio. The Pt and CePr active phases behave equal until 0.6 soot:catalyst weigh ratio and Pt performance was slightly better for higher soot loading. This difference is explaining according to the main soot combustion mechanisms occurring during Pt-DPF (NO_2-assited) and CePr-DPF regeneration (active oxygen). The CO_2 selectivity is near 100% for both catalysts in all the experimental reaction conditions evaluated. According to this study, the CePr active phase seems to be a promising candidate to replace Pt in real applications.

Keywords: Diesel soot; Diesel Particulate Filter; DPF; ceria catalyst; Pt catalyst.

ACCEPTED MANUSCRIPT

1.- INTRODUCTION.

The catalytic combustion of soot is a topic of current research in order to avoid the emissions of Diesel engines. One of the commercially available technologies consists of a Pt-based catalyst that oxidizes NO to NO_2 and initiates the combustion of soot collected in a Diesel Particulate Filter (DPF) located downstream in the exhaust pipe [1].

The high and fluctuating prize of noble metals has motivated the interest for alternative active phases, and ceria based-catalysts are promising candidates. Important progresses have been done at laboratory scale in the optimization of such ceria active phases. The effect of reaction conditions in the ceria-catalyzed combustion of soot, like gas composition or temperature windows for optimum operation, have been studied [2, 3] and the soot combustion mechanisms have been also properly investigated the most relevant reaction steps being understood [4, 5]. Even, some experiments at pilot plant level have been carried out in order to demonstrate that ceria-based formulations are able to accelerate soot combustion under real conditions [6-8].

The nature and amount of dopants loaded into the ceria framework has demonstrated to have a significant effect both in the thermal stability and catalytic activity for soot combustion of the ceria-based oxides. Most dopants studied are cations of d (Y [8], Zr [9-13], Hf [11], Nb [14], Mn [15], Ru [16], Zn [17], etc) and f (La [8, 9, 18, 19], Pr [8, 18, 19], Nd [19, 20], Sm [8, 18], Gd [21], Tb [18], etc) elements, and the most promising doped-ceria active phases seem to be those with Pr, Zr or La as main dopant.

The effect of the doped ceria synthesis method in the catalytic combustion of soot has also been deeply investigated. Straightforward methods

ACCEPTED MANUSCRIPT

like calcination of a metal precursors mixture or coprecipitation in alkali media have been studied, and also others more sophisticated synthesis pathways like surfactant-assisted methods, flame-spray synthesis, solid combustion synthesis with urea, sonochemical methods, carbon templating and citrate complexation synthesis among others [22-27]. It has been recently reported that ceria-praseodymia nanoparticles prepared by reversed microemulsion are able to outperform the soot combustion capacity of Pt in experiments performed with powder catalysts at laboratory scale [28].

In spite of all these advances done in the design of ceria-based soot combustion catalysts at laboratory, it is still necessary to compare the behavior of ceria-based and Pt active phases under realistic conditions in order to evaluate the potential substitution of noble metals in real applications, and the goal of the current study is to progress on this open question. One of the main handicaps in the study of soot combustion powder catalysts at laboratory is to mimic the soot-catalyst contact achieved inside a real filter, and for this reason Pt and an optimized ceria-based active phase have been loaded on DPFs filters in the current study. An experimental set-up has been designed to force a soot particles air suspension to pass through the DPFs, simulating the filtering process occurring in a real exhaust pipe. Also, the effect of important reaction parameters for a practical application have been studied, like the catalysts stability, the effect of the mass of soot loaded into the filters and the effect of H_2O and CO_2 together with NOx and O_2 in the reaction gas stream.

2.- EXPERIMENTAL DETAILS.

2.1. Commercial Diesel Particulate Filters (DPFs).

ACCEPTED MANUSCRIPT

Cylindrical SiC DPFs were supplied by CTI (Céramiques Techniques et Industrielles; France) and, according to CTI specifications, the composition is 90 % silicon carbide bound by inorganic oxides. A picture of one of these filters is shown in Figure 1. The incorporation of inorganic oxides to the formulation (mainly alumina) allows the further impregnation of catalytic active phases. Table 1 compiles some structural properties of the commercial DPFs substrates, as provided by the manufacturer.

2.2. Catalyst active phases loading into the DPFs.

Two active phases have been compared in this study, one being Pt and the other a complex copper oxide/ceria-praseodymia formulation optimized according to our previous experience, which has the nominal composition 10 wt. % (5%Cu/$Ce_{0.5}Pr_{0.5}O_2$) + 90 wt. % ($Ce_{0.5}Pr_{0.5}O_2$). These active phases were loaded on DPFs and the resulting samples are referred to as Pt-DPF and CePr-DPF, respectively. The active phase loading on the DPFs is 0.6 wt. % (≈ 6 $mg_{catalyst}/cm^3_{DPF}$) in both cases. In addition, a catalyst-free DPF has been used as reference, which is denoted by none-DPF. Considering the price we paid for all the chemicals used in the syntheses and for the DPFs, it is roughly estimated that the price of CePr-DPF is half to that of Pt-DPF.

2.2.1. Pt-DPF preparation.

The required amount of $Pt(NH_3)_4(NO_3)_2$ (Aldrich, 99.995%) was dissolved in the maximum amount of water (9 ml) that can be loaded into the DPF avoiding excess of solution dropping. Half of the platinum solution was dropped

ACCEPTED MANUSCRIPT

to one side of the DPF and the remaining half to the opposite side. In order to minimize the migration of the active phase solution into the DPF due to gravity, and therefore minimize the preferential accumulation of Pt in certain areas of the DPF, the impregnated DPF was dried while rotating in horizontal position. A warm air flow was used to heat the external walls of the DPF in order to speed up water evaporation (air does not flow through the DPF channels). Once dry, the Pt-DPF was calcined in static air at 500 ºC for 1 hour (heating rate 10 ºC/min).

2.2.2. CePr-DPF preparation.

The CePr-DPF was prepared in two steps. The first one consisted of 5%Cu/$Ce_{0.5}Pr_{0.5}O_2$ preparation and loading, the amount of 5%Cu/$Ce_{0.5}Pr_{0.5}O_2$ loaded being 10 wt. % of the total active phase mass. The copper-containing ceria-based active phases are highly active for CO oxidation to CO_2, therefore minimizing the emission of CO as undesired soot combustion by-product [29, 31] an also for NO oxidation to NO_2, which promotes the oxidation of soot at mild temperature (~350-450 ºC) [31]. However, copper impregnated on ceria hinders the oxidation of soot by the active oxygen mechanism, and for this reason, copper has only been impregnated in 10% of the whole ceria-based active phase, therefore keeping the remaining 90% free of copper.

For 5%Cu/$Ce_{0.5}Pr_{0.5}O_2$ preparation, the required amounts of $Ce(NO_3)_3{\cdot}6H_2O$ (Aldrich, 99.9%) and $Pr(NO_3)_3{\cdot}6H_2O$ (Aldrich, 99.9%) were mixed in a mortar and calcined in air at 500 ºC for 2h (with a heating rate of 10 ºC/min). Then, $Cu(NO_3)_2{\cdot}3H_2O$ (Panreac, 99% purity) was loaded by incipient wetness impregnation with a water solution and the powder was further calcined

ACCEPTED MANUSCRIPT

in static air at 500 ºC for 2 hours (with a heating rate of 10 ºC/min). An ethanol suspension of the resulting active phase was prepared using Triton X-100 (polioxiethylene (9) 4 –(1,1,3,3,-tetramethybutyl) phenyl ether) as surfactant (50 ml ethanol + 10 ml triton for one DPF) and ultrasounds were applied for 30 min to favors dispersion. The active phase loading into the monolith was done immediately after the ultrasounds treatment by using the device whose scheme is shown in Figure 2. Half of the suspension was poured to one side of the DPF, and afterwards, the position of the monolith was changed up-side-down and the remaining half suspension was poured to the other side. As shown in Figure 2, vacuum was used to force the active phase to enter into the SiC structure and for solvent removal. Then, the DPF was dried overnight in static air at 100 ºC. It has to be noted that the solvent collected after the active phase loading was completely transparent (the active phase suspension was red) and that the incorporation of the desired amount of active phase was gravimetrically confirmed.

The second step consisted of the preparation and loading of $Ce_{0.5}Pr_{0.5}O_2$, the amount being in this case 90 wt. % of the total active phase mass. This active phase was previously optimized and was able to outperform the behavior of a commercial Pt catalyst in laboratory experiments performed with powder catalysts tested in loose contact under a $NOx + O_2 + N_2$ flow [28]. A reversed microemulsion method was used to prepare $Ce_{0.5}Pr_{0.5}O_2$-nanoparticles precursor micelles, which was previously reported [28]. In brief, the required amounts of Ce and Pr precursors were dissolved in water and a microemulsion was prepared in n-heptane, including Triton X-100 as surfactant and hexanol as co-surfactant. A similar microemulsion was prepared but with

ACCEPTED MANUSCRIPT

tetramethylammonium hydroxide instead of the metal precursors. Both microemulsions were mixed and vigorously stirred for 24 hours. This suspension of micelles was loaded into the DPF (which already contains 5%Cu/$Ce_{0.5}Pr_{0.5}O_2$) by also using the Figure 2 device and following the same procedure previously described. In this case, the micelles suspension was not completely clean after passing one time throughout the DPF (half suspension for each DPF side), and the process was repeated for 3 times until the solvent collected was apparently clean. Finally, the CePr-DPF was dried overnight in air at 100 ºC and calcined in air at 500 ºC for 1 hour (heating rate 10ºC/min). The desired active phase loading was also gravimetrically confirmed.

2.3. Catalytic tests.

DPFs regeneration experiments were carried out in the experimental setup schematized in Figure 3. This set up consists of a stainless steel horizontal reactor with two thermocouples placed inside, one upstream and the other downstream the DPF. An additional third thermocouple, which is not plotted on Figure 3, was used for furnace temperature control. A set of gas cylinders and mass flow controllers was used to prepare the reactive gas mixtures, which in most cases consisted of 500 ml/min of 500 ppm NOx + 5 %O_2 in N_2. Some experiments were also performed with the same total flow but additionally including 4 % CO_2 and 2 % H_2O. The gas composition was continuously monitored by NDIR-UV gas analyzers (BINOS series, by Fisher-Rosemount) for CO, CO_2, NO, NO_2 and O_2.

In a typical experiment, a DPF was placed into the reactor and valves 1 and 3 (see Figure 3) were kept open while valves 2 and 4 remained closed in

ACCEPTED MANUSCRIPT

order to force an air stream to pass through the DPF due to the action of a vacuum pump. Then, the desired amount of soot (Printex U) was fed, as indicated in the Figure 3, being collected in the DPF. Most experiments were carried out with 50 mg of soot, otherwise indicated. Once soot was loaded into the DPF, valves 1 and 3 were closed, valves 2 and 4 were open in order to allow the reactive gas mixture to flow through the reactor and the temperature was raised at 10 ºC/min from room temperature to 800 ºC.

The soot conversion profiles were determined from CO and CO_2 evolved, and the carbon mass balances were closed with an average experimental error of 10%.

2.4 SEM-chemical mapping characterization.

After the catalytic tests, the used DPFs were cut and observed by SEM in a HITACHI S-3000N microscope equipped with an X-ray detector (XFlash 3001 de Bruker) for chemical mapping. An automatic stainless steel circular blade (2 cm diameter), a 1 mm-thickness stainless steel bar and a hammer were used to cut the DPFs avoiding degradation of the active phases coating in the SEM observation area.

The DPFs were placed in vertical position to be cut. The stainless steel bar was placed on the top side of the DPFs and each DPF was cut in two half cylinders giving a hummer beat to the stainless steel bar. To force the DPFs breakdown in two perfect half cylinders, and not in many non-uniform pieces, marks were done to the DPFs with the circular blade before the hammer beat. Two vertical ~ 0.5 mm-deep marks were made on the external surface of the

ACCEPTED MANUSCRIPT

DPFs. Both marks were parallel to the monolith channels, were separated to each other as much as possible and had the length of the entire DPF (7.5 cm). An additional mark was also made on the top side of the DPFs joining the extremes of both vertical marks, and the result is an up-side-down "U" shape mark. The stainless steel bar was placed on this top mark to be beaten by the hammer. Finally, the half cylinders were cut in approximately 3 cm length pieces by using the circular blade in order to fit into the SEM chamber.

3.- RESULTS AND DISCUSSION.

3.1. Catalysts characterization.

Figure 4 shows SEM images of the three DPFs. The none-DPF filter (Figure 4b) shows grey SiC particles of around 25 μm glued together with a binder, keeping an open structure with voids to allow the gas to flow trough. The catalyst-containing DPFs also show the described SiC open structure, but the active phases are additionally observed.

The CePr active phase is clearly shown on Figure 4b as white particles located into the SiC particles network, and it is interesting to pay attention to the distribution of this active phase into the DPF. Most area of the Figure 4b shows the surface of one channel, and a detail of a perpendicular wall can be seen on the right-hand side of the image. The white spots of the CePr phase are only located on the flat horizontal SiC surface, but not inside the perpendicular right-hand side wall. This means that this active phase was mainly deposited on the surface of the SiC walls, and not inside the porous SiC particles network.

ACCEPTED MANUSCRIPT

Pt particles are not so evident on Figure 4c, and a zoom in image (see inset) was necessary to identify white Pt spots on the surface of the gray SiC particles. Considering that the amount (in wt. %) of Pt and CePr active phases loaded on Pt-DPF and CePr-DPF respectively was the same, it would be expected that the amount of active phases observed on Figures 4b and 4c is also more or less the same. Nevertheless, this is not the case and much more CePr is observed on Figure 4b than Pt on Figure 4c. The reason is that, opposite to that observed for CePr, Pt is not only located on the surface of the SiC walls but also inside the porous SiC particles network. The different distribution of both active phases inside the DPFs is tentatively attributed to the fact that the platinum precursor dissolution used to impregnate the Pt-DPF is expected to enter into the SiC porous network much better than both the 5%Cu/$Ce_{0.5}Pr_{0.5}O_2$ particles and the $Ce_{0.5}Pr_{0.5}O_2$-nanoparticles precursor micelles suspensions.

Chemical analysis was used to confirm the nature of the particles observed by SEM, and Figures 5 (CePr-DPF) and 6 (Pt-DPF) show SEM images of selected areas (Figures 5a and 6a, respectively) together with the corresponding chemical mapping for Ce (Figure 5b), Pr (Figure 5c) and Pt (Figure 6b). Copper (and any other metal) was not detected by this technique due to its very low concentration.

These chemical analyses confirm that the white particles observed in the SEM images correspond to the active phases. In case of the CePr-DPF (Figure 5), the regions with high Ce (Figure 5b) and Pr (Figure 5c) concentration are the same, which was expected considering that the preparation methods used to prepare the CePr active phase force the formation of mixed oxides.

ACCEPTED MANUSCRIPT

3.2. Catalytic tests.

3.2.1. Comparison of Pt-DPF and CePr-DPF.

Several consecutive soot combustion experiments were carried out with the different filters under 500 ppm NOx + 5% O_2 + N_2 flow, and the soot conversion profiles obtained from CO and CO_2 evolved are compiled in Figure 7. Also, the CO_2 selectivity values (CO_2 evolved with regard to total CO + CO_2) are included in Table 2.

These experiments evidence that, in the one hand, the experimental procedure used for soot loading into the filters (see Figure 3 and text for details) allows obtaining very reproducible soot conversion curves, and on the other hand, both catalyst-containing filters are stable with no evidences of catalysts deactivation after the second run. It is worth to mention that the behavior of both catalytic filters during the first soot combustion experiment (not shown to simplify the figure) is different to that on further cycles, which is attributed to changes in the active phases the first time they are exposed to the reaction conditions.

The catalytic activity of the CePr active phase is similar to that of Pt, and also the selectivity towards CO_2 formation, which is almost 100% in both cases. Note that the CO_2 selectivity in the uncatalysed reaction was 51 %, evidencing the catalytic effect of the active phases.

These results obtained with DPF-supported catalysts are consistent with those previously obtained with powder catalysts and soot:catalyst mixtures prepared in loose contact [28], where $Ce_{0.5}Pr_{0.5}O_2$ nanoparticles prepared by a

ACCEPTED MANUSCRIPT

microemulsion method showed even better activity than a commercial 1%Pt/alumina catalyst.

3.2.2. Effect of the mass of soot.

The effect of the amount of soot loaded into the filters was studied, because this is an issue of practical relevance to determine how often the filter must be regenerated. It is expected that the amount of soot loaded affects the contact between soot and catalyst particles, since the first soot particles loaded have more chances to be in touch with catalyst particles than particles loaded afterwards. Also, the mass of soot loaded can potentially affect the temperature into the filter during the highly exothermal combustion. However, evidences of an uncontrolled increase of temperature was not observed in any experiment performed in this study, as deduced from the temperature profiles recorded by the DPF upstream and downstream thermocouples that follow the expected heating ramp.

Figure 8 shows results of the experiments performed with different mass of soot. Figure 8a and 8b include the soot conversion profiles obtained with CePr-DPF and Pt-DPF, respectively, and Figure 8c is a plot of the T50% temperatures, which is the temperature required for 50% soot combustion, as a function of the soot:catalyst weight ratio at the beginning of each experiment. In addition, Table 2 compiles the CO_2 selectivity values, which are near 100% for all mass of soot studied.

The mass of soot has no effect on the soot conversion profiles for low soot:catalyst ratios (weigh ratio below 0.4; mass of soot ≤ 50 mg), and this means that there is a linear relationship between mass of soot and soot conversion rate, the higher the mass the faster the rate, suggesting a first order

ACCEPTED MANUSCRIPT

kinetics with regard to soot mass. Nevertheless, the soot conversion profiles are delayed to slightly higher temperatures for soot:catalyst weigh ratios above 0.4 (experiments with more than 50 mg of soot) for both catalytic filters, and this could be a consequence of the difficult soot-catalyst contact. The behavior of both catalytic filters is equal until 0.6 soot:catalyst weight ratio, but Pt-DPF is slightly more active for the highest ratio tested (soot:catalyst weight ratio = 1; mass of soot = 180 mg). This could be related to the different soot combustion mechanisms occurring on Pt-DPF and CePr-DPF. Pt-catalyzed soot combustion occurs following the NO_2-assisted mechanism, that is, Pt oxidizes NO to NO_2 and NO_2, which is much more oxidizing than NO and O_2, initiates the combustion [32]. The CePr active phase also promotes this NO_2-assisted mechanism, but is less active than Pt for NO oxidation to NO_2 [28]. Additionally, ceria-catalysts oxidize soot by the so-called active oxygen mechanism, which consists of the exchange of oxygen atoms between the ceria catalysts and the O-containing gases (O_2 is the most abundant one) producing active oxygen species that are highly active for soot combustion. The main handicap of this active oxygen mechanism is that active oxygen species must be transferred from the ceria catalyst to soot particles, otherwise they recombine to each other and yield O_2, and the soot-catalyst contact plays a key role in such transfer process [33]. The results of Figure 8 suggest that the active oxygen mechanism occurring on CePr-DPF, which is based on short-lifetime active oxygen species, is hindered for high soot loading more than the NO_2-assisted mechanism. This is because the NO_2 lifetime is long enough to reach the soot particles even if they are far away from the catalyst, but not active oxygen lifetime. This would

ACCEPTED MANUSCRIPT

explain why Pt is more effective for filter regeneration than the CePr active phase for high mass of soot loading.

3.2.3. Effect of H_2O + CO_2.

Finally, the effect of H_2O + CO_2 in the DPFs regeneration has been studied, because it is known from experiments performed with powder catalysts that both H_2O and CO_2 can affect the catalytic combustion of soot [3]. The soot conversion profiles obtained with Pt-DPF and CePr-DPF both under NOx + O_2 + N_2 and NOx + O_2 + H_2O + CO_2 + N_2 are compared in Figure 9, showing that the soot conversion profiles are slightly delayed towards higher temperatures in the presence of H_2O + CO_2. This delay affects in a quite similar extent to both catalysts, with shifts in the T50% temperatures of 18 and 12 ºC for Pt-DPF and CePr-DPF respectively. The CO_2 selectivity values shown in Figure 2 are also near 100% in the presence of H_2O + CO_2. These promising results confirm that the CePr active phase is able to oxidize soot as fast as Pt under the realistic conditions of these experiments.

4.- Conclusions.

The catalytic regeneration of Diesel Particulate Filters has been studied, comparing the behavior of Pt and a CePr active phase. It is concluded that:

- The preparation procedures used lead to the accumulation of the CePr active phase mainly on the surface of the DPF channels while Pt is distributed more homogeneously into the porosity of the SiC particles network.

ACCEPTED MANUSCRIPT

- Both active phases (Pt and CePr) are stable under reaction conditions, with no evidences of deactivation in consecutive combustion experiments.
- The mass of soot loaded into the filters has no effect in the catalytic regeneration for soot:catalyst weigh ratios below 0.4, while it is hindered above this ratio. The Pt and CePr active phases behave equal until 0.6 soot:catalyst weigh ratio and Pt performance is slightly better for higher soot loading. This difference is explaining according to the main soot combustion mechanisms occurring during Pt-DPF (NO_2-assited) and CePr-DPF regeneration (active oxygen).
- The presence of H_2O and CO_2 together with NOx and O_2 in the gas mixture slightly delays soot combustion to higher temperatures, but the effect is equal for the Pt and CePr active phases.
- The CO_2 selectivity is near 100% for both catalysts in all the experimental reaction conditions evaluated.
- The CePr active phase seems to be a promising candidate to replace Pt is real applications.

Acknowledgments

The financial support of Generalitat Valenciana (Project PROMETEOII/2014/010)), Spanish Ministry of Economy and Competitiveness (Project CTQ2012-30703) and UE (FEDER funding) is acknowledged.

References

[1] M. V. Twigg, Appl. Catal. B 70 (2007) 2-15.

ACCEPTED MANUSCRIPT

[2] M.A. Peralta, V.G. Milt, L.M. Cornaglia, C.A. Querini, J. Catal. 242 (2006) 118–130.

[3] A. M. Hernández-Giménez, D. Lozano-Castelló, A. Bueno-López. Appl. Catal. B 148–149 (2014) 406–414.

[4] A. Setiabudi, J. Chen, G. Mul, M. Makkee, J. A. Moulijn. Appl. Catal. B 51 (2004) 9–19.

[5] N. Guillén-Hurtado, A. García-García, A. Bueno-López. J. Catal. 299 (2013) 181–187.

[6] J. Lahaye, S. Boehm, Ph. Chambrion, Ph. Ehrburger. Comb. Flame 104 (1996) 199–207.

[7] P. C. de Sousa Filho, L. F. Gomes, K. T. de Oliveira, C. R. Neri, O. A. Serra. Appl. Catal. A 360 (2009) 210–217.

[8] K. Krishna, A. Bueno-López, M. Makkee, J. A. Moulijn, Appl. Catal. B 75 (2007) 189-200.

[9] L. Katta, P. Sudarsanam, G. Thrimurthulu, B. M. Reddy, Appl. Catal. B 101 (2010) 101-108.

[10] I. Atribak, A. Bueno-López, A. García-García, J. Catal. 259 (2008) 123-132.

[11] E. Aneggi, C. de Leitenburg, J. Llorca, A. Trovarelli, Catal. Today 197 (2012) 119-126.

[12] V. Sánchez Escribano, E. Fernández López, J. M. Gallardo-Amores, C. del Hoyo Martínez, C. Pistarino, M. Panizza, C. Resini, G. Busca, (2008) Comb. Flame 153 (2012) 97-104.

[13] C. A. Neyertz, E. D. Banús, E.E. Miró, E.E., C. A. Querini, Chem. Eng. J. 248 (2014) 394-405.

[14] M. Casapu, A. Bernhard, D. Peitz, M. Mehring, M. Elsener, O. Kröcher, Appl. Catal. B 103 (2011) 79-84.

[15] X. Wu, F. Lin, H. Xu, D. Weng, Appl. Catal. B 96 (2010) 101-109.

[16] M. Kurnatowska, W. Mista, P. Mazur, L. Kepinski, Appl. Catal. B 148-149 (2014) 123-135.

[17] L .F Nascimento, R. F. Martins, R.F. Silva, R.F., O. A. Serra, J. Env. Sci. (China) 26 (2014) 694-701.

[18] E. Aneggi, C. de Leitenburg, G. Dolcetti, A. Trovarelli, Catal. Today 114 (2006) 40-47.

[19] P. Dulgheru, J. A. Sullivan, Top. Catal. 56 (2013) 504-510.

ACCEPTED MANUSCRIPT

[20] A. M. Hernández-Giménez, L. P. dos Santos Xavier, A. Bueno-López, Appl. Catal. A 462-463 (2013) 100-106.

[21] D. N. Durgasri, T. Vinodkumar, B. M. Reddy, B.M. J. Chem. Sci. 126 (2014) 429-435.

[22] D. Terribile, A. Trovarelli, J. Llorca, C. de Leitenburg, G. Dolcetti, Catal. Today 43 (1998) 79-88.

[23] W. J. Stark, M. Maciejewski, L. Mädler, S. E. Pratsinis, S.E., Baiker, J. Catal. 220 (2003) 35-43.

[24] J. C. Yu, L. Zhang, J. Lin. (2003) J. Colloid Int. Sci. 260, 240–243.

[25] M. Crocker, U. M. Graham, R. Gonzalez, G. Jacobs, E. Morris, A. M. Rubel, R. Andrews, J. Mater. Sci. 42 (2007) 3454-3464.

[26] C. Bozo, F. Gaillard, N., Guilhaume, Appl. Catal. A 220 (2001) 69-77.

[27] I. Atribak, A. Bueno-López, A. Garcia-Garcia, Catal. Commun. 9 (2008) 250–255.

[28] N. Guillén-Hurtado, A. García-García, A. Bueno-López. Appl. Catal. B 174 (2015) 60–66.

[29] A. Martínez-Arias, J. Soria, R. Cataluña, J. C. Conesa, J.V. Cortés Corberán. Stud. Surf. Sci. Catal. 116 (1998) 591-600.

[30] L. P. dos Santos Xavier, V. Rico-Pérez, A. M. Hernández-Giménez, D. Lozano-Castelló, A. Bueno-López. Appl. Catal. B 162 (2015) 412–419.

[31] J. Giménez-Magrogil, A. Bueno-López, A. García-García. Appl. Catal. B 152–153 (2014) 99–107.

[32] A. Setiabudi, B. A.A.L van Setten, Michiel Makkee, J. A Moulijn. Appl. Catal. B 35 (2002) 159–166.

[33] B.A.A.L. van Setten, J.M. Schouten, M. Makkee, J.A. Moulijn, Appl. Catal. B 28 (2000) 253-257.

ACCEPTED MANUSCRIPT

ACCEPTED MANUSCRIPT

FIGURE CAPTIONS

Figure 1. Picture of the commercial SiC DPFs substrates used in this study.

Figure 2. Scheme of the experimental setup used to load the CePr active phase loading.

Figure 3. Scheme of the experimental setup used to perform the catalytic tests.

Figure 4. SEM images of (a) None-DPF, (b) CePr-DPF and (c) Pt-DPF.

Figure 5. Chemical mapping of CePr-DPF. (a) SEM image, (b) Cerium concentration map and (c) Praseodymium concentration map.

Figure 6. Chemical mapping of Pt-DPF. (a) SEM image and (b) Platinum concentration map.

Figure 7. Effect of the catalysts in filters regeneration in a 500 ppm NOx + 5% O_2 + N_2 stream (all experiments in this figure were performed with 50 mg of soot).

Figure 8. Effect of the mass of soot in the filters regeneration in a 500 ppm NOx + 5% O_2 + N_2 stream. (a) CePr-DPF and (b) Pt-DPF. (c) comparison of T50% temperatures (temperatures required for 50% soot conversion).

Figure 9. Effect of H_2O + CO_2 in the catalytic regeneration of filters (all experiments in this figure were performed with 50 mg of soot and a gas streams with 500 ppm NOx + 5% O_2 + N_2 or 500 ppm NOx + 5% O_2 + 2% H_2O + 4% CO_2 + N_2).

ACCEPTED MANUSCRIPT

ACCEPTED MANUSCRIPT

Table 1. Structural properties of the commercial DPF substrates.

Diameter	2.3 cm
Length	7.5 cm
Open porosity	46 %
Mean pore size	20 µm
Cell Density	300 cpsi
Wall thickness	30 mm
Substrate density	1.62 g/cm^3
Filtration area	0.98 cm^2/cm^3

Table 2. CO_2 selectivity with regard to total COx evolved in soot combustion experiments performed with different filters, mass of soot and gas mixture.

Filter	mass of soot (mg)	Gas mixture	CO_2 selectivity (%)
None-DPF	50	NOx + O_2 + N_2	51
CePr-DPF	10	NOx + O_2 + N_2	93
CePr-DPF	25	NOx + O_2 + N_2	94
CePr-DPF	50	NOx + O_2 + N_2	96
CePr-DPF	100	NOx + O_2 + N_2	95
CePr-DPF	50	NOx + O_2+ CO_2 + H_2O+ N_2	94
Pt-DPF	10	NOx + O_2 + N_2	97
Pt-DPF	50	NOx + O_2 + N_2	98
Pt-DPF	100	NOx + O_2 + N_2	96
Pt-DPF	50	NOx + O_2+ CO_2 + H_2O+ N_2	99

According to reproducibility experiments, the experimental error in the CO_2 selectivity values is estimated to be ± 3 %.

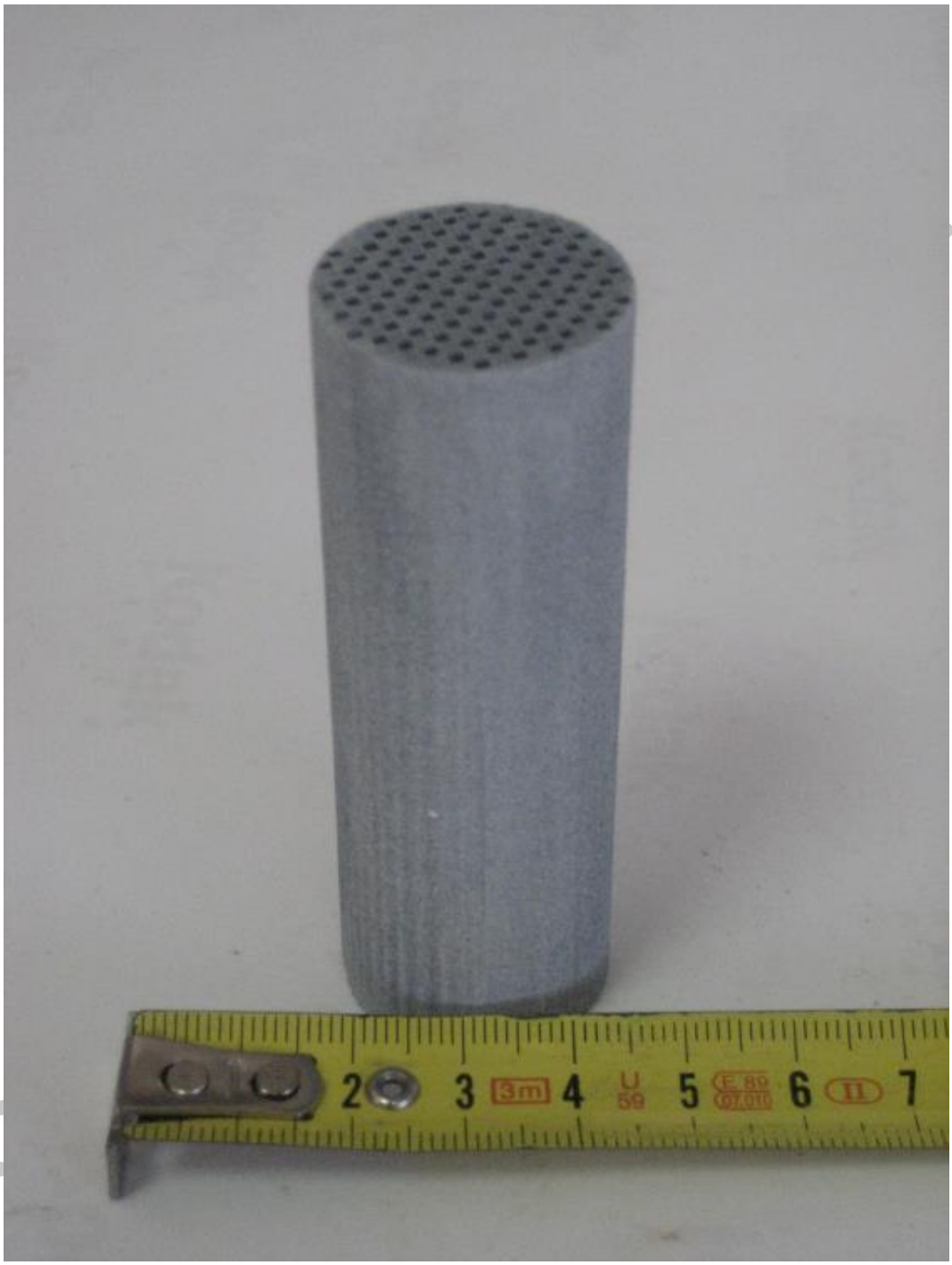

Figure 1

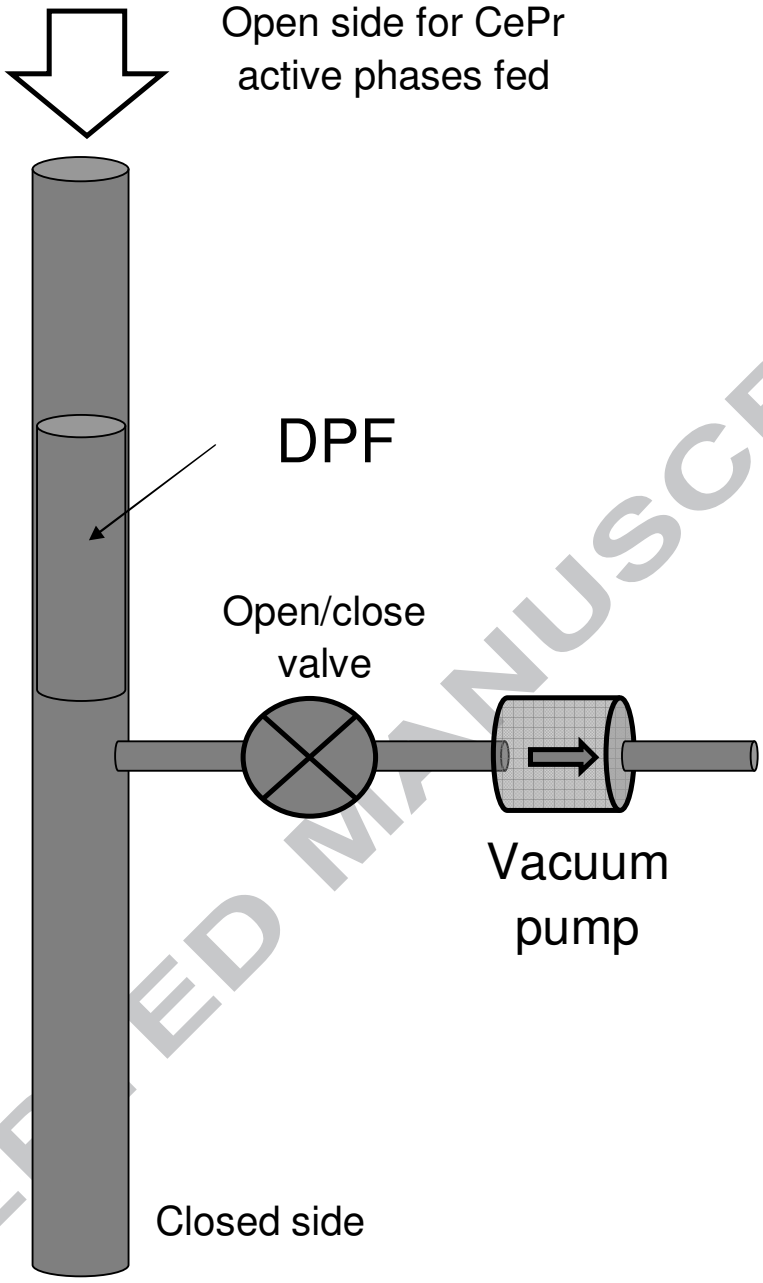

Figure 2

ACCEPTED MANUSCRIPT

ACCEPTED MANUSCRIPT

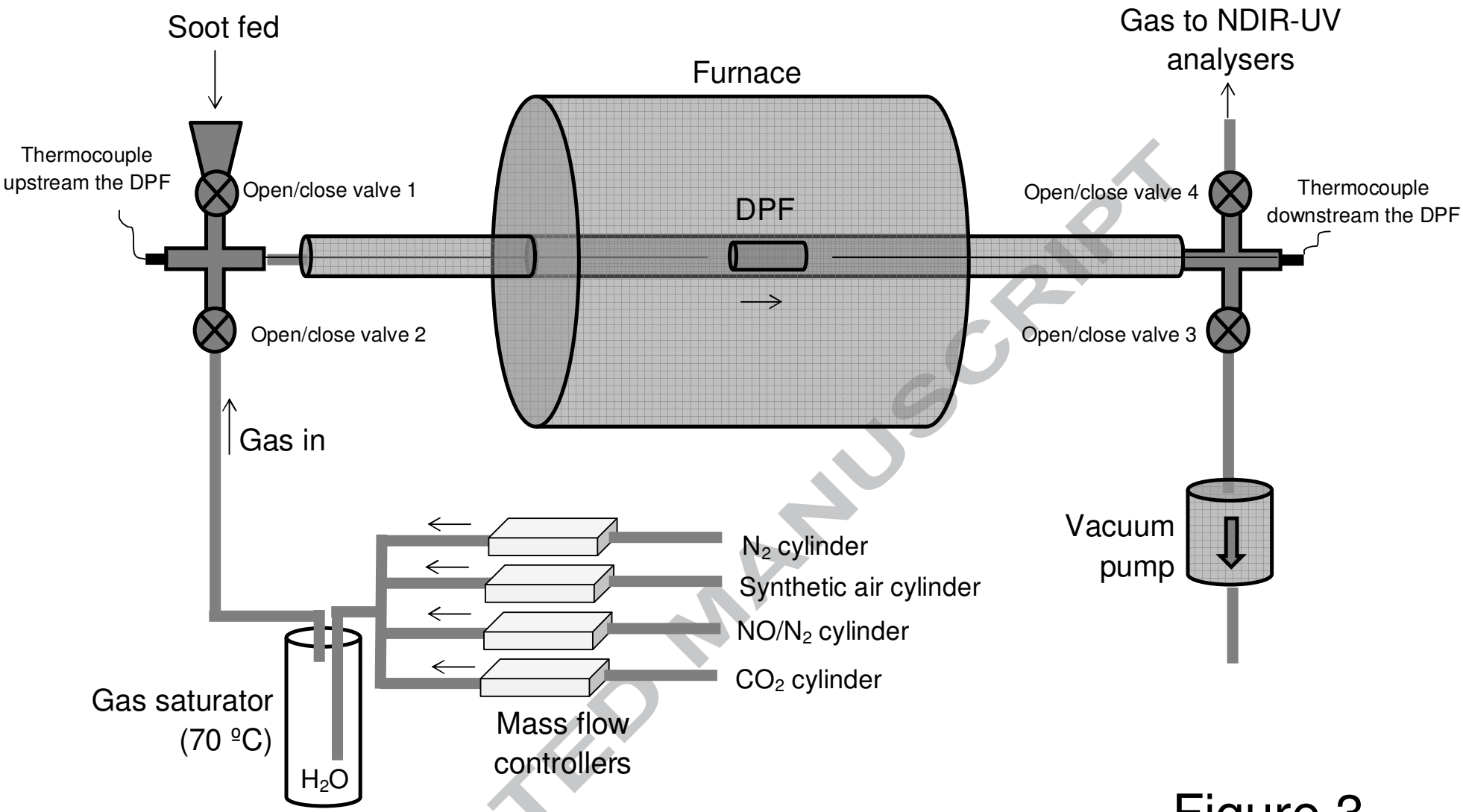

Figure 3

ACCEPTED MANUSCRIPT

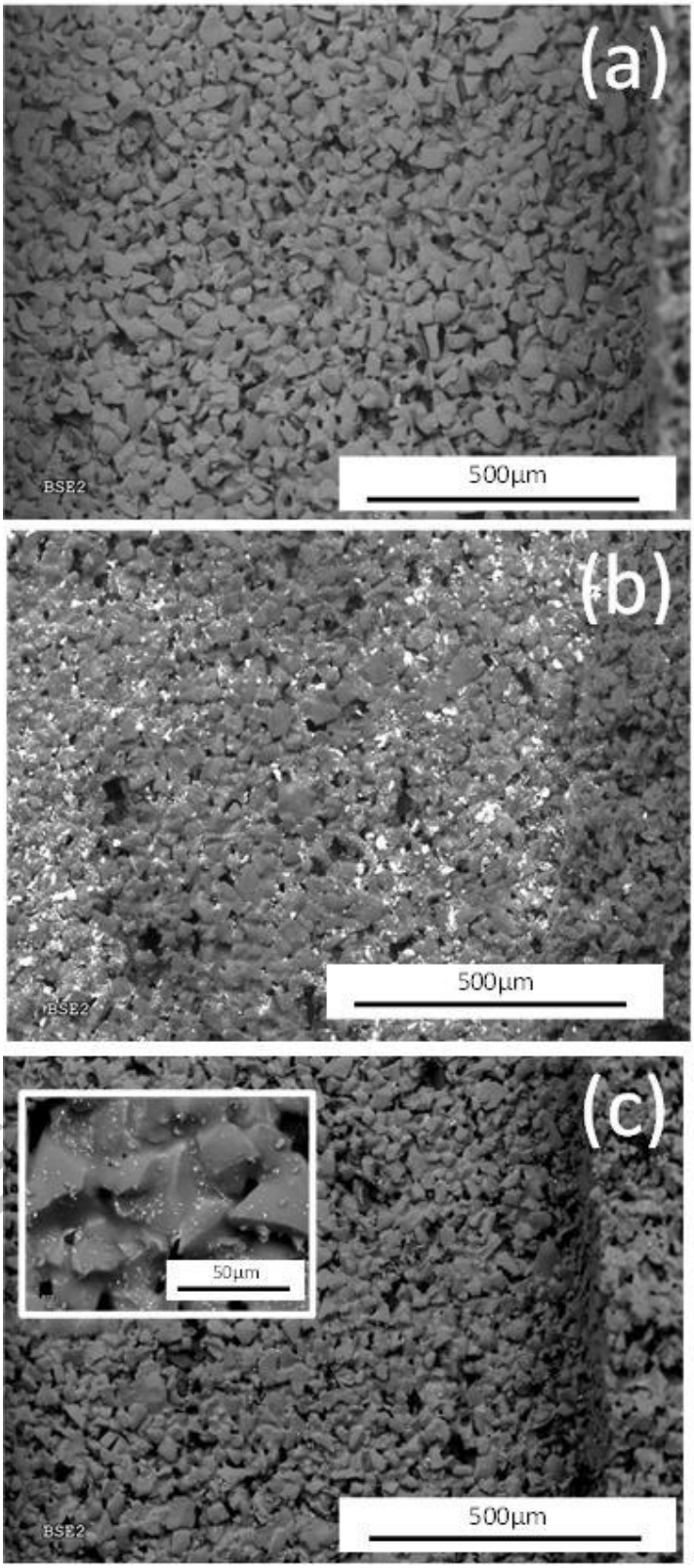

Figure 4

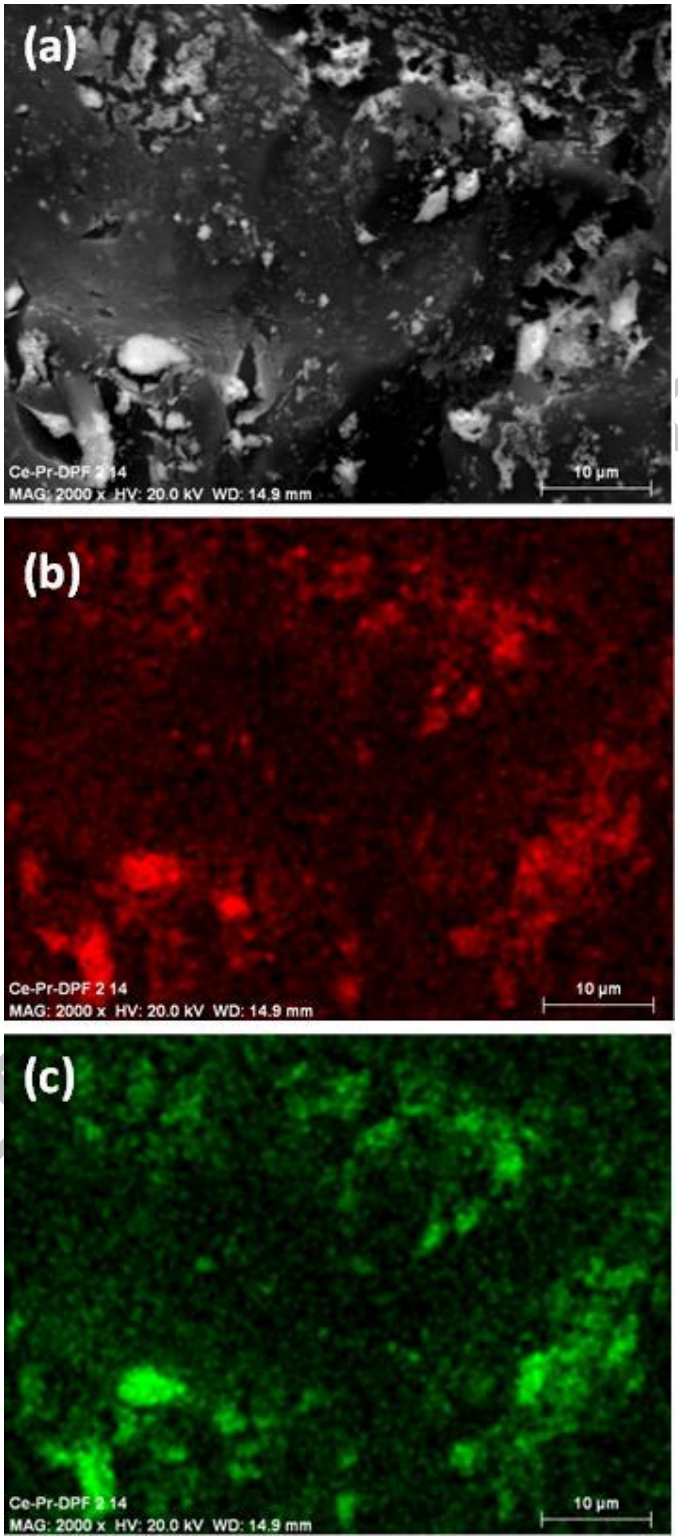
(a)
Ce-Pr-DPF 2 14
MAG: 2000 x HV: 20.0 kV WD: 14.9 mm
10 µm
(b)
Ce-Pr-DPF 2 14
MAG: 2000 x HV: 20.0 kV WD: 14.9 mm
10 µm
(c)
Ce-Pr-DPF 2 14
MAG: 2000 x HV: 20.0 kV WD: 14.9 mm
10 µm

Figure 5

ACCEPTED MANUSCRIPT

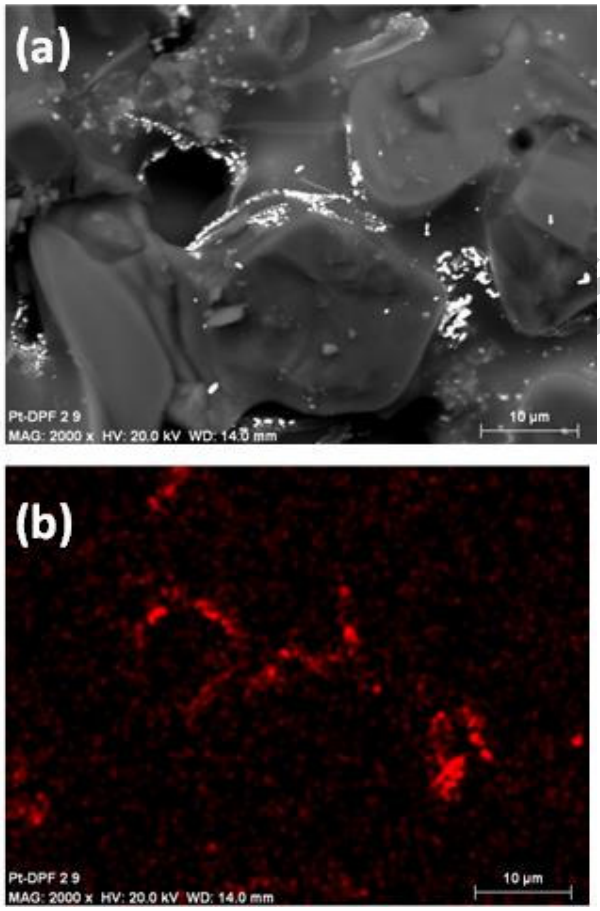

Figure 6

ACCEPTED MANUSCRIPT

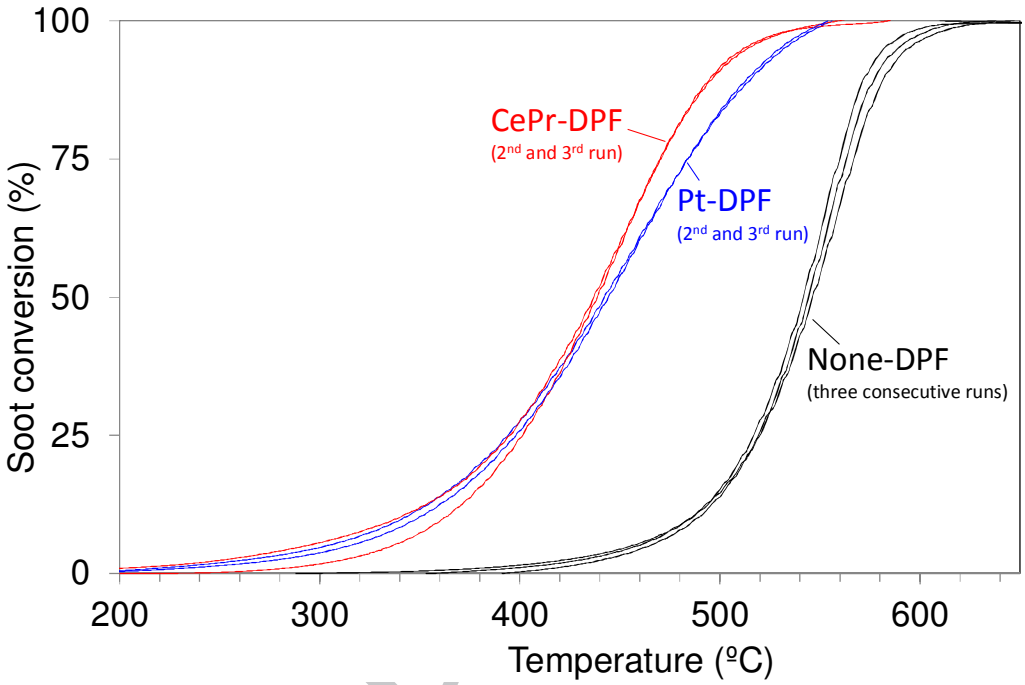

Figure 7

ACCEPTED

ACCEPTED MANUSCRIPT

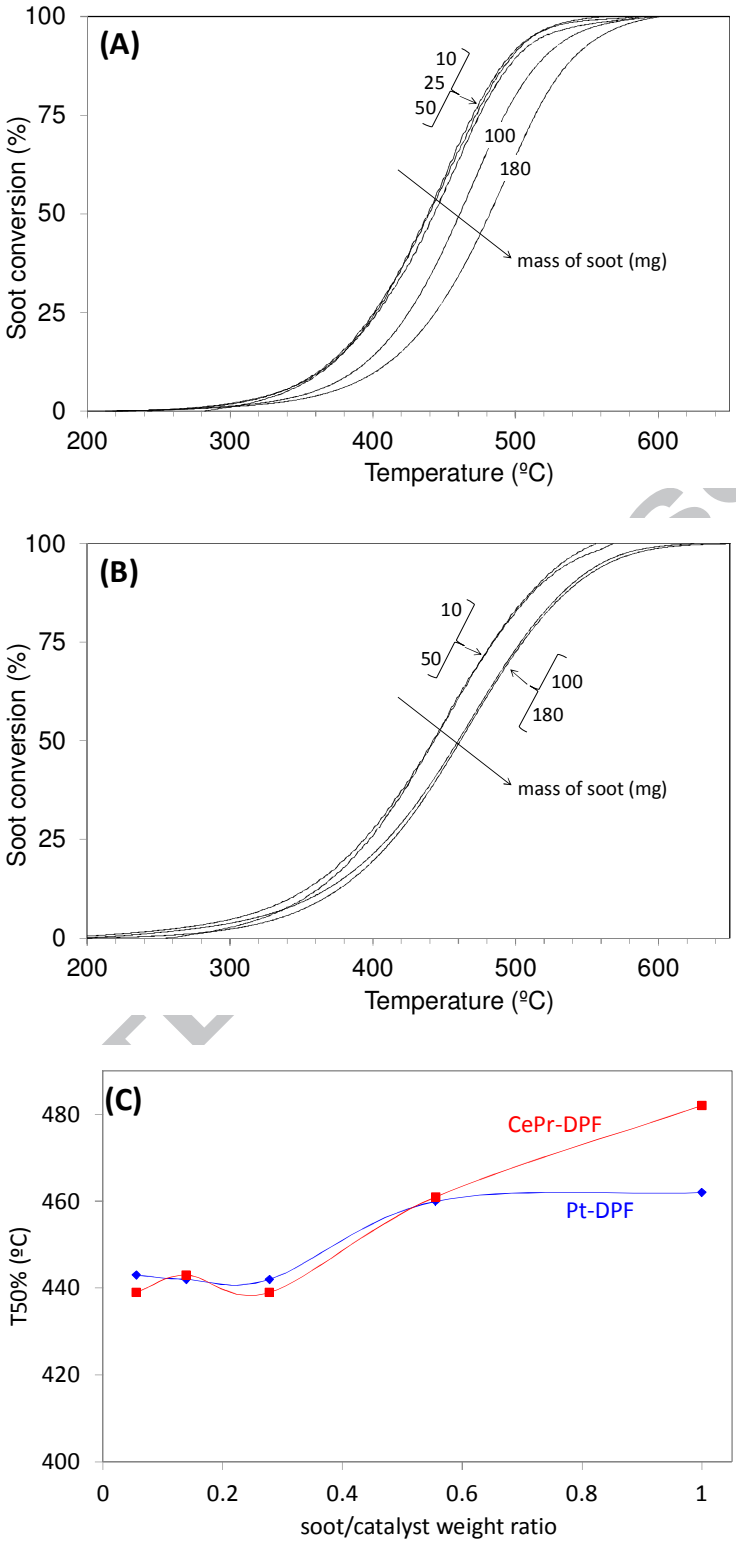

Figure 8

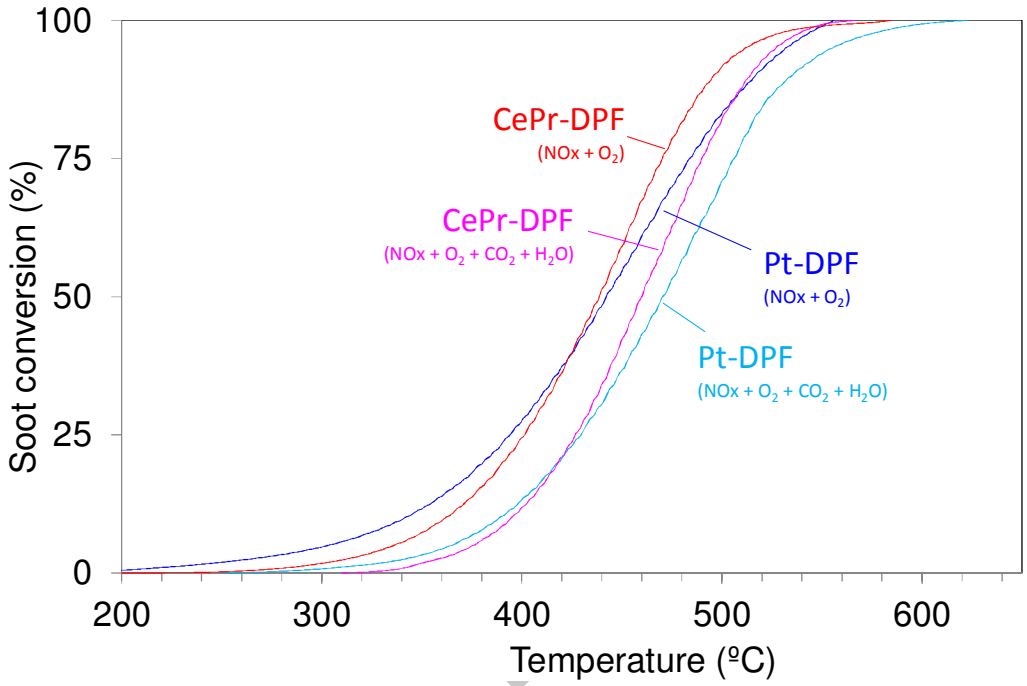

Figure 9

ACCEPTED

ACCEPTED MANUSCRIPT

Graphical abstract

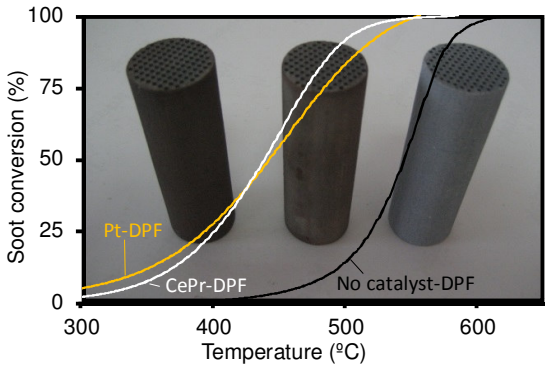

ACCEPTED MANUSCRIPT

ACCEPTED MANUSCRIPT

Highlights

- DPFs have been loaded with 0.6 wt. % of either Pt or an optimized CePr active phase
- Pt-DPF and CePr-DPF are regenerated at equal temperature in most conditions
- Both Pt and CePr active phases are stable after several DPF regeneration cycles
- The presence of H_2O and CO_2 affects equally to Pt-DPF and CePr-DPF
- CePr is a promising candidate to replace Pt in real soot removal DPFs

ACCEPTED MANUSCRIPT